TRIASSIC-JURASSIC RIFT-RELATED DEFORMATION AND TEMPERATURE-TIME EVOLUTION OF THE FOSSIL ADRIATIC MARGIN: A REVIEW FROM OSSOLA AND STRONA DI OMEGNA VALLEYS (IVREA-VERBANO ZONE)

Matteo Simonetti*, Antonio Langone *,✉, Stefania Corvò*, and Mattia Bonazzi*,****

* *Institute of Geosciences and Earth Resources, National Research Council (C.N.R.), Pavia, Italy.*
** *Department of Earth and Environmental Sciences, University of Pavia, Italy.*
✉ *Corresponding author, e-mail: langone@crystal.unipv.it*

Keywords: *geochronology; thermochronology;Ivrea-Verbano Zone; Anzola shear zone; Forno-Rosarolo shear zone; Tethyan rifting; Adriatic Margin.*

ABSTRACT

The direct observation and investigation of rift-related structures at the mesoscale is uncommon. Hence, detailed constraints on the evolution of the main faults and shear zones developed during crustal extension are not always available.

The Ivrea-Verbano Zone, in the Italian Southern Alps, samples remnants of the former lower crust of the rifted margins surrounding the Alpine Tethys and therefore provides the opportunity to directly investigate rift-related tectonics. Here, several shear zones have been recognized and interpreted as related to Mesozoic rifting. However, even if there is a general agreement with this interpretation, the precise age of activity of many of those shear zones is not well constrained.

In this paper we present a review of the Triassic-Jurassic geochronological and thermochronological data available for two sections of the Ivrea-Verbano Zone, the Strona di Omegna and Ossola valleys, where at least two extensional shear zones are exposed. Ductile deformation occurred under amphibolite-facies conditions and it was alternatively attributed to late Variscan deformation or to Triassic-Jurassic rifting-related tectonics.

We discuss the available chronological data and the different interpretations provided for the shear zones considering also new geochronological studies on other lower crustal shear zones exposed in other sectors of the Ivrea-Verbano Zone. This review allows us to strengthen the more recent interpretations indicating that these shear zones are important tectonic structures related to Late Triassic-Jurassic deformation in the lower crust of the Adriatic margin.

INTRODUCTION

Several tectonic processes can lead to strain accumulation within the lithosphere. Strain is often localized into shear zones that show large variations in orientation, length, thickness, displacement, strain geometry, deformation regime and deformation mechanisms, all depending from the tectonic framework in which they form (e.g., Fossen and Cavalcante, 2017). Therefore, the study of shear zones may provide valuable information relevant to unravel the evolution of many geodynamic contexts. Because the complex nature of shear zones leads to a great variability in their evolution, a modern approach to the study of such structures requires the combination of many independent techniques, in order to unravel their kinematics, deformation temperatures, deformation regimes and strain geometry (see also Sibson, 1977; Law et al., 2004; Xypolias, 2010; Law, 2014). Furthermore, several geochronometers can be used to constrain the age and duration of deformation. Such multidisciplinary approach in the last years provided important constraints for new tectonic models in several collisional settings all over the world (Iacopini et al., 2008; Montomoli et al., 2013; Zhang et al., 2013; Iaccarino et al., 2015; Giorgis et al., 2017; Wu et al., 2017; Carosi et al., 2018; 2020; Parsons et al., 2018; Simonetti et al., 2020a; 2020b). The combination of geophysical, structural, geochronological and sedimentological studies also led to important advancement in understanding extensional tectonics, rift settings and related structures (Manatschal et al., 2007; Mohn et al., 2010; 2012; Beltrando et al., 2014; 2015; Aravadinou and Xypolias, 2017; Langone et al., 2018; Real et al., 2018; Petri et al., 2019).

Studies of rifted margins, in the last decade, benefited from an increasing quantity of high-quality data from several disciplines. However, the direct observation and investigation of rift-related structures at the mesoscale is uncommon. Detailed constraints on the evolution of the main faults and shear zones developed during crustal extension are not always available even, if they would be fundamental data to elucidate this process and to constrain the rifting models.

Rift systems are generally subjected to shift in time and space within the evolving continental margins (Manatschal et al., 2007; Mohn et al., 2012; Beltrando et al., 2015). This is the case of the Mesozoic evolution of Southern Europe and North Africa where multiple rifting episodes characterize the Pangea breakup. Indeed, the Middle Triassic opening of the Meliata and Ionian Basins (Kozur, 1991; Speranza et al., 2012) was followed by the formation of the central Atlantic and the Alpine Tethys in the latest Triassic to Middle Jurassic times.

Extension-related tectonics began in the Late Triassic (Bertotti et al., 1993). During this epoch, extension of the upper crust was mainly controlled by major listric faults, such as the Lugano Val Grande fault, at the margins of Late Carboniferous-Early Permian basins. Subsequently, faulting around those centres gradually ceased and the site of extension shifted westwards towards the future site of crustal separation.

Manatschal et al. (2007), Mohn et al. (2012) and Beltrando et al. (2015) documented the rift-related evolution of the basement and the associated tectono-sedimentary record. According to their studies, three modes can be recognized during Tethyan rift localization. An initial stretching mode (mode 1) characterized by a ductile and diffused deformation of the middle and deep crust is followed by a thinning mode (mode 2) linked to initial rift localization and lithospheric thinning and, finally, by an exhumation mode (mode 3) where the crustal extension leads to a complete exhumation of the subcontinental mantle. During the three modes of Tethyan rift, several generations and types of extensional structures are formed, namely high-angle and low-angle normal faults, anastomosing shear-zones and decoupling horizons (Petri et al., 2019). Such structures accommodate the lateral extraction of mechanically stronger levels derived from the middle and lower crust. The first extensional ductile shear zones in the lower crust nucleates during the thinning mode (mode 2 of Manatschal et al. 2007) that is the less constrained stage among the three. Direct geological observations are not so common mainly because the fault systems and the sedimentary basins related to this mode are overprinted by subsequent, breakup-related deformation.

The Ivrea-Verbano Zone (IVZ) and the Serie dei Laghi (SdL) couple, in the Italian Southern Alps, samples remnants of the former Alpine Tethys rifted margin and therefore provides the opportunity to investigate rift-related tectonics across different crustal levels. In particular, the IVZ-SdL couple is interpreted as the Adriatic necking zone recording major thinning during Jurassic rifting (Decarlis et al., 2017). Instead, the Adriatic distal domain is preserved in the Canavese Zone, which shows evidence for subcontinental mantle exhumation at the seafloor (Ferrando et al., 2004; Beltrando et al., 2015).

Several shear zones have been recognized in the IVZ (e.g., Rutter et al., 1993), where two major sets of structures are interpreted as related to Mesozoic rifting (Petri et al., 2019). The first set consists of high-temperature shear zones, whereas the second one consists of lower temperature fault structures. In the SdL, the Pogallo Line (PL), which in places marks the contact with the IVZ, is interpreted as a low-angle normal fault active under lower temperature conditions (Hodges and Fountain, 1984; Schmid et al., 1987; Zingg et al., 1990) compared to the shear zones within the IVZ (middle rift-related structures of Petri et al., 2019).

Even if there is a general agreement in considering all those structures linked to crustal extension, the precise age of activity of many of them is not well constrained and locally a detailed structural analysis is lacking. This leads to unclear correlations between similar structures that crops out in different localities of the IVZ and to the lack of precise structural and temporal constraints about the activity of such shear zones and faults. Because of these uncertainties, the reconstruction of exhumation and rifting processes is still limited and partly unclear.

The first step toward a complete understanding of the role of the shear zones in the IVZ during rifting process is a complete revision of the geochronological and thermochronological data available in the literature. In this paper we present a detailed review and discussion of available geochronological and thermochronological data, with a focus on the Triassic-Jurassic time interval, for two sections of the IVZ exposed along the Strona di Omegna and Ossola valleys. Here, two shear zones, namely the Forno-Rosarolo and the Anzola shear zones respectively, are exposed. These two mylonitic belts have been recently interpreted as belonging to the same system of shear zones affecting the northern sector of the IVZ, formed during the rifting process (middle rift-related structures of Petri et al., 2019). The aim of this paper is to verify which of the data already available in literature can be indicative of the period of activity of these structures, in order to strengthen their correlation and to better understand their role in the framework of Tethyan rifting.

GEOLOGICAL SETTING

The IVZ is located in northwestern Italy and belongs to the South Alpine domain (Fig. 1). It represents an exposed section of the pre-Alpine middle to lower continental crust that escaped a marked Alpine deformation overprint. It is separated from the Sesia Zone by the Insubric Line to the northwest and from the SdL by the Late-Variscan Cossato-Mergozzo-Brissago Line (CMB) and, in places, by the Pogallo Line (PL) to the southeast (Boriani et al., 1990). The CMB Line is crosscut by mylonites associated with the PL (Fig. 1), which is interpreted as a low-angle normal fault of Triassic-Jurassic age (Zingg et al., 1990) linked to crustal thinning (Hodges and Fountain, 1984). During the Alpine collision, the IVZ underwent exhumation and verticalization (Henk et al., 1997; Rutter et al., 2007; Wolff et al., 2012) together with the development of large-scale folds, such as the Proman antiform (Brodie and Rutter, 1987).

The IVZ is traditionally divided, from NW-SE, in three units: the mantle peridotites, the Mafic Complex and the Kinzigite Formation (Fig. 1). The main bodies of mantle peridotites are the Finero, Balmuccia, and Baldissero massifs that crop out close to the Insubric Line (Hartmann and Wedepohl, 1993). The Mafic Complex was emplaced during Permian (Peressini et al., 2007) with underplating relations and is coeval with the acid magmatism and volcanism recognized in the upper crust (Karakas et al., 2019). The bimodal magmatism is interpreted as an evidence for thinned lithospheric mantle (Schuster and Stüwe, 2008). The main phase of basic magmatism occurred at 288±4 Ma (e.g., Peressini et al. 2007) and probably started largely before, as suggested by the presence of mafic sills emplaced during Carboniferous (e.g., ~ 314; Klötzli et al., 2014). According to Klötzli et al. (2014), the overlapping ages, within error, between these old magmatic events and the high-temperature regional metamorphism (~ 316 Ma; Ewing et al., 2013; 2015) documents a link between high grade metamorphism and magmatism. The Kinzigite Formation is made up of metasedimentary rocks with intercalated metabasic rocks (Zingg, 1990; Schmid, 1993). The metamorphic grade increases toward the NW (Schmid and Wood, 1976; Zingg, 1983) from amphibolite- to granulite-facies. In particular, the SE part of the Kinzigite Formation consists of micaschists that recorded amphibolite-facies metamorphism, intercalated with amphibolite layers, whereas to the NW felsic and mafic granulites (also known as stronalites) are present. Lenses of calcsilicates and marbles are more abundant within the amphibolite-facies rocks but also occur within the granulites. Considering the changes in the mineral assemblage along the Strona di Omegna section, some authors introduced a further subdivision of the Kinzigite Formation with a transition zone between amphibolite- and granulite-facies metamorphic rocks (e.g., Redler et al., 2012; Kunz et al., 2014). In both the Ossola and Strona di Omegna valleys, the transition from amphibolite- to granulite-facies is marked by mylonitic zones: the Anzola shear zone (Brodie

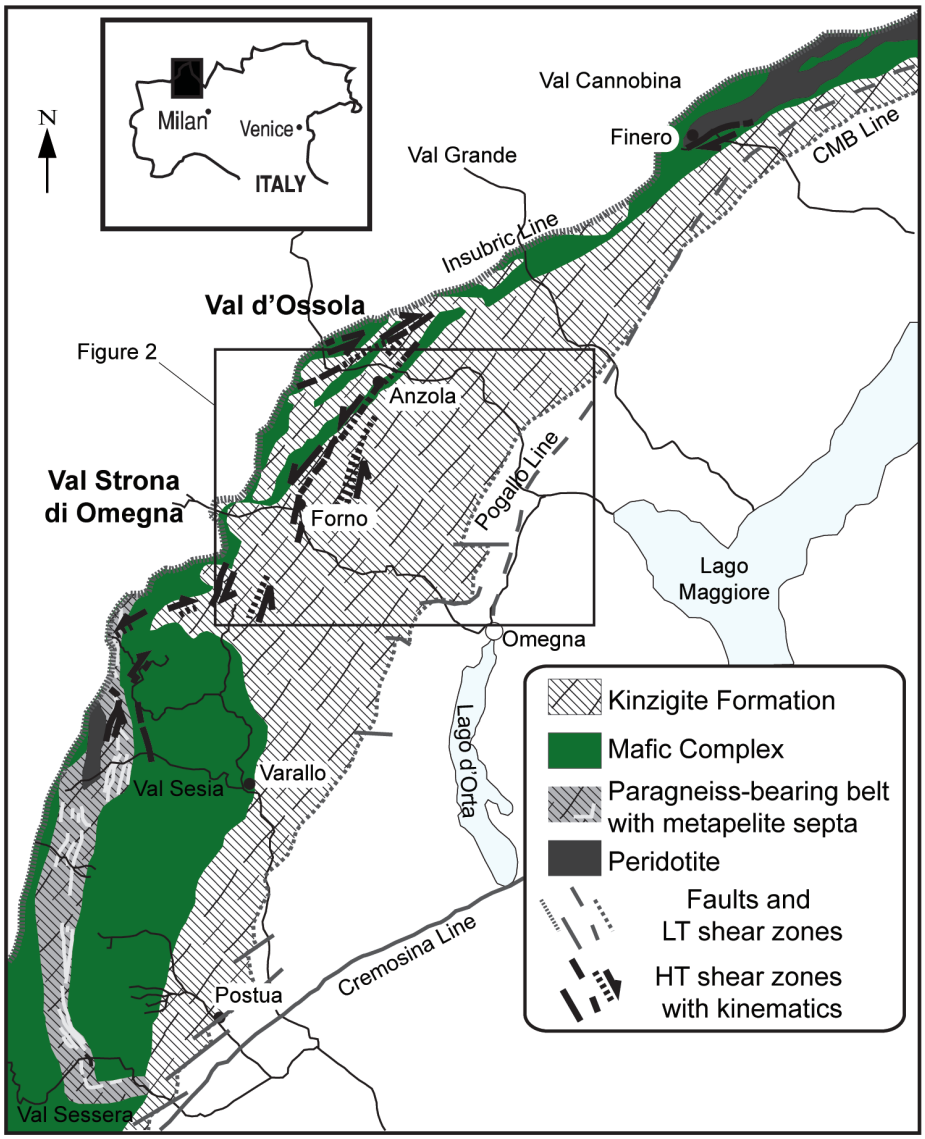

Fig. 1 - Geological sketch map of the central and northern IVZ (=Ivrea Verbano Zone, modified after Ewing et al., 2015). The locations of high-temperature shear zones are after Rutter et al. (1993).

and Rutter, 1987) and the Rosarolo shear zone (Siegesmund et al., 2008), respectively. These structures were typically associated to a single fault system named in different way: the Anzola-Rosarolo (Beltrando et al., 2015) or Anzola-Forno shear zone (Ewing et al., 2015). In this work, we refer to the high strain zone in the Ossola valley as the Anzola shear zone (Fig. 2A), whereas the high strain zone in the Strona di Omegna valley is referred to as Forno-Rosarolo shear zone (Fig. 2B).

From the structural point of view, the metamorphic foliation of the IVZ strikes NE-SW and is generally steeply inclined with a mineral lineation plunging toward SE. A system of large-scale superimposed folds linked to Variscan deformation is also recognized (Rutter et al., 2007). From the paleogeographic point of view, the IVZ was located to the western edge of the Adriatic Plate (Manatschal et al., 2007; Mohn et al., 2012; Beltrando et al., 2015). It was involved in a complex and polyphase episode of rift focusing in the Triassic-Jurassic interval that was investigated by integrating geochronological and thermochronological tools with available tectonostratigraphic records (Beltrando et al., 2015 and references therein).

THE LATE/POST VARISCAN HIGH-TEMPERATURE DEFORMATION

Following the Variscan orogeny, the IVZ was affected by post-orogenic extension (as testified by the activity of the CMB during Permian) and subsequently, in the Triassic-Jurassic time interval, by a complex and polyphase episode of rift focusing (Beltrando et al., 2015). The post-Variscan deformation was recognized since the earlier studies of the IVZ (Brodie and Rutter, 1987; Boriani et al., 1990; Rutter et al., 1993; 2007; Siegesmund et al., 2008; Garde et al., 2015). Crustal extension was accommodated by several shear zones active during different phases of rifting (Manatschal et al., 2007; Mohn et al., 2012) at different crustal levels (e.g., Beltrando et al., 2015). The uppermost rifting-related structure is the PL, which formed in the Kinzigite Formation and is interpreted as a low-angle shear zone with a normal kinematics (Hodges and Fountain, 1984) active between 210 and 170 Ma (Zingg, 1990; Wolff et al., 2012) under decreasing temperatures from amphibolite- to greenschist-facies conditions. New data about the extensional structures affecting the lower crust have been recently obtained from the northern sector of the

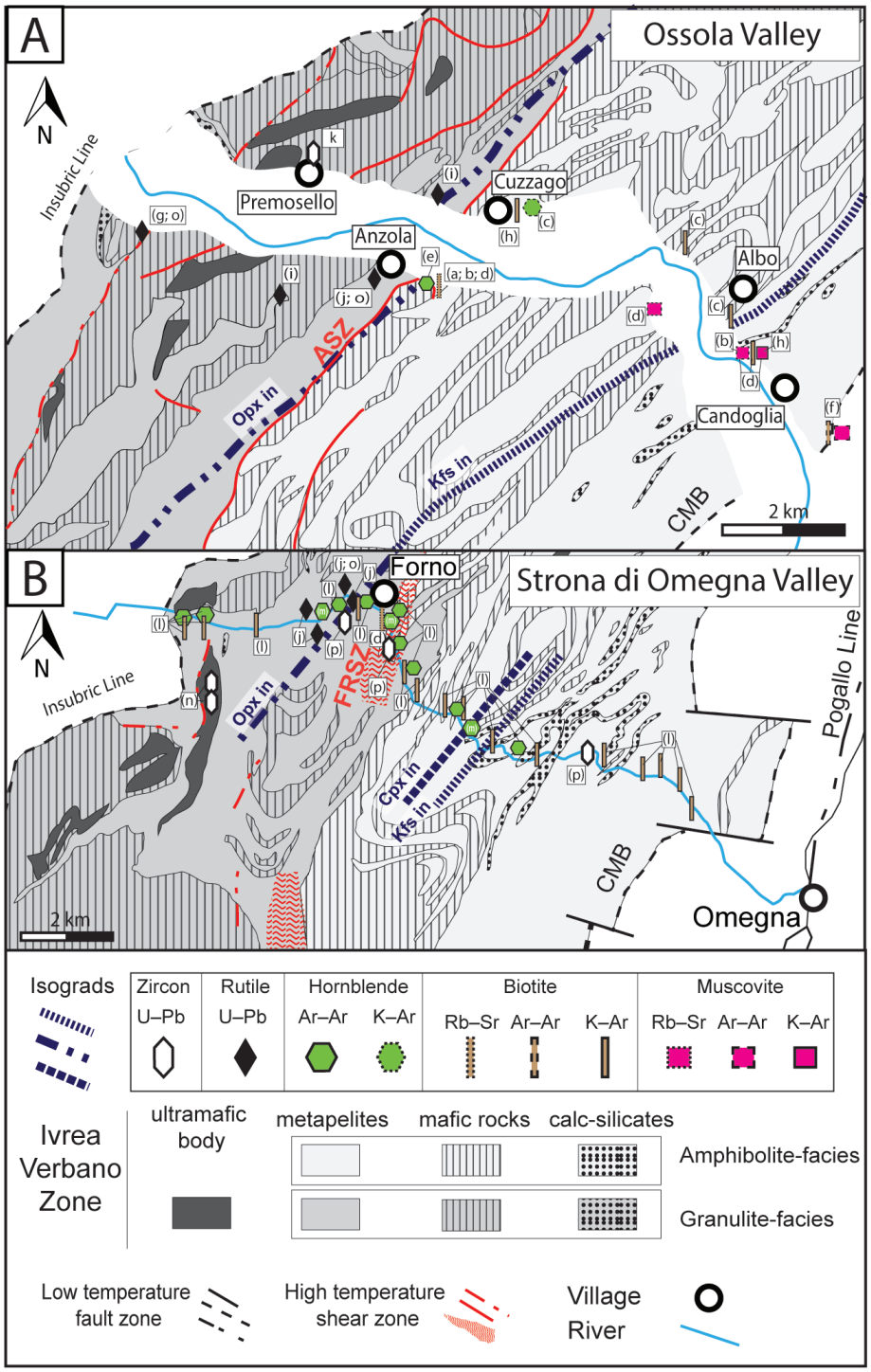

Fig. 2 - Schematic geological maps showing the main lithologies, tectonic structures and isograds, for Ossola (A) and Strona di Omegna (B) valleys, modified after Rutter et al. (2007). Isograds for the Ossola valley are from Zingg (1980) whereas for the Strona di Omegna valley isograds are from Redler et al. (2012) for metapelitic rocks (Kfs in) and Kunz et al. (2014) for the metabasic rocks (cpx and opx in). ASZ- Anzola shear zone; FRSZ- Forno-Rosarolo shear zone; CMB- Cossato-Mergozzo-Brissago Line. The published Triassic-Jurassic radiometric data are located according to the relative reference (lowercase letters) with a symbol referring to the adopted mineral and/or isotopic system. References: a- Jäger et al., 1967; b- Graeser and Hunziker, 1968; c- McDowell and Schmid, 1968; d- Hunziker, 1974; e- Brodie et al., 1989; f- Mulch et al., 2002; g- Zack et al., 2011; h- Wolff et al 2012; i- Smye and Stockli, 2014; j- Ewing et al., 2015; k- Kusiak et al., 2019; l- Siegesmund et al., 2008; m- Boriani and Villa, 1997; n- Denyszyn et al., 2018; o- Smye et al., 2019; p- Vavra et al., 1999.

IVZ (Langone et al., 2018; Corvò et al., 2020). Here, ductile shear zones affecting mafic/ultramafic rocks (Fig. 1) were active in a large time interval, from Late Triassic to Early Jurassic (see also Boriani and Villa, 1997) and from granulite- to greenschist-facies conditions (Brodie, 1981; Altenberger, 1995; Kenkmann, 2000; Kenkmann and Dresen, 2002; Degli Alessandrini, 2018; Langone et al., 2018). In the central part of the IVZ (Fig. 2), where the Strona di Omegna and Ossola valleys are located, rift-related deformation is probably represented by the Forno-Rosarolo (Siegesmund et al., 2008) and the Anzola shear zones (Brodie and Rutter, 1987), whose main characteristics are briefly described in the following sections.

The Anzola shear zone

The Anzola shear zone is exposed in a quarry 500 m east of Anzola village in the Ossola valley (Fig. 2A). It is approximately 20 metres wide and shows a vertical foliation, which strikes NNE-SSW, slightly discordant to the metamorphic layering of the surrounding unsheared rocks (Fig. 2A; Stünitz, 1998). This structure was the focus of several works (Brodie, 1981; Brodie and Rutter, 1987; Brodie et al., 1989; Rutter and Brodie, 1990; Rutter et al., 1993; Altenberger, 1997; Stünitz, 1998; Rutter et al., 2007) because it gives an excellent opportunity to study shear localiza-

tion within amphibolite-facies mafic rocks at middle/lower crustal levels. Brodie (1981) was the first author focusing on the shear zone, and investigated the role of deformation during metamorphism and its effects on mineral and rock chemistry. The author demonstrated that the composition of amphibole and plagioclase, varies with deformation suggesting recrystallization under increasing temperature (prograde regional metamorphism). The microstructural and geochemical evolution of the shear zone was further investigated by Stünitz (1998). The Author showed that syn-tectonic recrystallization of clinopyroxene, amphibole and plagioclase produce compositional differences between porphyroclasts and recrystallized grains. In particular, the Author observed that: i) recrystallized clinopyroxene is characterized by higher Mg# value (Mg/Mg + Fe) and Al content with respect to the porphyroclasts; ii) recrystallized grains of hornblende tend to have lower Ti content and higher Mg# value; iii) recrystallized plagioclase has lower anorthite and orthoclase components with respect to the rare plagioclase porphyroclasts. Combining microstructures with chemical changes Stünitz (1998) concluded that deformation took place during a retrograde P-T path under amphibolite-facies conditions (from ~ 650 to 550°C) at pressures of probably less than 8 kbar. The Anzola shear zone was studied also by Altenberger (1997) who revealed that the pre-existing heterogeneity (i.e., layering and grain-size variations) was the *locus* of concentrated shear deformation. As already documented by Brodie (1981), Altenberger (1997) further highlighted that mylonitic layers are richer in amphiboles than the wall rocks.

Despite the numerous studies on the microstructural and geochemical evolution of the shear zone the P-T conditions, i.e. prograde for Brodie (1981) and retrograde for Stünitz (1998), as well the timing are still unconstrained. The work of Brodie et al. (1989) is the first attempt to constrain the age of the deep crustal extensional episode in the Ossola valley. The authors provided Ar-Ar radiometric dating of hornblende from the undeformed gabbros and mylonites, their results are reported in the geochronological review section (IV.I; Table 1).

The Forno-Rosarolo shear zone

In the last decades the Strona di Omegna valley (Fig. 2B), has been widely studied from several point of view since it offers a spectacular exposure of continental crustal rocks for a thickness of ~ 14 km (the largest thickness of the Kinzigite Formation for the IVZ). Despite the high strain zone between Forno and Rosarolo villages was documented since Rutter et al. (1993) and subsequently studied by several authors (Rutter et al., 2007; Siegesmund et al., 2008; Garde et al., 2015), a complete characterization of the deformation characteristics and precise constraints about its geometry and internal structure are lacking. In addition, the deformation age was not directly constrained by *in situ* dating of syn-tectonic minerals and/or overgrowths. Zircon grains from a mylonitic sample from the Forno-Rosarolo shear zone was dated by Kunz et al. (2018) and provided two age populations with an overall range of U-Pb dates from 316 to 264 Ma. However, since the dated zircon domains do not show evidence of deformation-induced recrystallization, these ages do not provide information about the timing of shearing. The lack of robust geochronological constraints prevents to frame the activity of this shear zone within the complex large-scale post-Variscan geodynamic context.

According to Siegesmund et al. (2008), the Forno-Rosarolo shear zone can be described as a high-strain zone made up of a network of sub-parallel anastomosing shear zones variable from centimetric to metric scale. The authors proposed that the shear zone operated over a long-time span and that it initiated during the Early Permian magmatic underplating by accommodating extension in the lower crust under high-temperature conditions. Subsequently the shear zone was reactivated at different crustal levels during Mesozoic tectonics and was involved into Eocene tilting together with the whole IVZ (Siegesmund et al., 2008). During its long-lasting activity, the shear zone experienced both cataclastic and ductile deformation but due to the rheological contrast between individual layers made of different rock types, brittle and ductile deformation may have operated simultaneously, at least in some cases. Evidences of brittle deformation are cataclastic zones with centimetric to metric thickness oriented parallel to the shear zone boundary (Siegesmund et al., 2008).

The late stage of activity of the Forno-Rosarolo shear zone was associated with the intrusion of a network of mafic dykes that cut the mylonitic foliation or, in places, form sills oriented parallel to it (Siegesmund et al., 2008). These fine-grained mafic rocks were recently interpreted as cataclastic injectites by Garde et al. (2015). According to these authors, cataclasis began with disperse general comminution followed by localized comminution, especially of garnet, and fluidization. The latter induced the formation of very fine-grained multi-layered dykes a few centimetres thick, which may cut back into the cataclastic fractures. Interestingly, the authors recognized that these brittle deformation features together with other evidences (such as pseudotachylites) were similar to impact-related structures observed in other contexts.

GEOCHRONOLOGICAL REVIEW: THE TEMPERATURE-TIME HISTORY

The available petrological, geochronological and thermochronological data for the IVZ reflect a complex thermal history after the Permian intrusion of the Mafic Complex (e.g., Siegesmund et al., 2008; Wolf et al., 2012; Ewing et al., 2013; 2015; Smye and Stockli, 2014; Smye et al., 2019). The Temperature-time (T-t) history is characterized by alternating cooling and (re)heating episodes linked to the main geodynamic events. In particular, the IVZ crustal section preserves thermal evidence for lithospheric thinning, Jurassic extension, continental breakup (e.g., Ewing et al., 2013; 2015; Smye and Stockli, 2014; Beltrando et al., 2015; Smye et al., 2019), as well as for exhumation of the crustal section in conjunction with the Alpine orogenesis (e.g., Zingg et al., 1990). Although these episodes are broadly recognized and even if there is a general agreement that the IVZ suffered exhumation, cooling and heating episodes during Jurassic, there are currently only a few constraints on the activity of ductile shear zones between Late Triassic and Early Jurassic in lower crustal rocks. In the following sections we summarize the available geochronological data (Fig. 3; Tables 1 and 2) for the shear zones and surrounding host rocks for both the Ossola and Strona di Omegna valleys. In the T-t diagrams of Fig. 3, the radiometric data and relative errors are coupled with temperatures as provided by the authors or as reported in previous T-t reconstructions (e.g., Schmid et al., 1987; Brodie et al., 1989; Zingg et al., 1990; Siegesmund et al., 2008; Smye and Stockli, 2014; Ewing et al., 2015).

Table 1 - Representative compilation of Triassic-Jurassic geochronological data available for the Ossola valley.

Dating method	Mineral	Rock type	Metamorphic facies	Age±error (Ma)	Locality	Reference
$^{206}Pb/^{238}U$	zircon	mylonititc stronalite	granulite	245±10	Premosello	Kusiak et al., 2019*
$^{206}Pb/^{238}U$	zircon	mylonititc stronalite	granulite	239±4	Premosello	Kusiak et al., 2019*
$^{206}Pb/^{238}U$	zircon	mylonititc stronalite	granulite	235±10	Premosello	Kusiak et al., 2019*
$^{206}Pb/^{238}U$	zircon	mylonititc stronalite	granulite	230±10	Premosello	Kusiak et al., 2019*
$^{206}Pb/^{238}U$	zircon	mylonititc stronalite	granulite	221±3	Premosello	Kusiak et al., 2019*
$^{206}Pb/^{238}U$	zircon	mylonititc stronalite	granulite	185±6	Premosello	Kusiak et al., 2019*
$^{206}Pb/^{238}U$	zircon	mylonititc stronalite	granulite	181±3	Premosello	Kusiak et al., 2019*
U–Pb concordia age	rutile	stronalite	granulite	181±4	Loro	Zack et al. 2011
$^{206}Pb/^{238}U$	rutile	stronalite	granulite	184.4±4.6	Megolo	Smye and Stockli, 2014
$^{206}Pb/^{238}U$	rutile	stronalite	granulite	187.4±7.6	Megolo	Smye and Stockli, 2014
$^{206}Pb/^{238}U$	rutile	stronalite	granulite	171±5	Premosello	Ewing et al, 2015
$^{206}Pb/^{238}U$	rutile	stronalite	granulite	155±5	Premosello	Ewing et al, 2015
$^{206}Pb/^{238}U$	rutile	stronalite	granulite	187±3-155±12	Anzola	Smye et al., 2019
$^{206}Pb/^{238}U$	rutile	stronalite	granulite	187±3-177±3	Loro	Smye et al., 2019
$^{40}Ar–^{39}Ar$	hornblende	mafic granulite	granulite	284.27±5.56	Anzola	Brodie et al., 1989
$^{40}Ar–^{39}Ar$	hornblende	mafic granulite	granulite	224.11±4.31	Anzola	Brodie et al., 1989
$^{40}Ar–^{39}Ar$	hornblende	mafic granulite	granulite	217.98±4.15	Anzola	Brodie et al., 1989
$^{40}Ar–^{39}Ar$	biotite	metapelite	amphibolite/greenshist	123.3±7.2	Mergozzo	Mulch et al., 2002
$^{40}Ar–^{39}Ar$	muscovite	metapelite	amphibolite/greenshist	147.7±5.1	Mergozzo	Mulch et al., 2002
$^{40}Ar–^{39}Ar$	muscovite	metapelite	amphibolite/greenshist	147.3±6.5	Mergozzo	Mulch et al., 2002
$^{40}Ar–^{39}Ar$	muscovite	metapelite	amphibolite/greenshist	182.7±2.4	Mergozzo	Mulch et al., 2002
$^{40}Ar–^{39}Ar$	muscovite	metapelite	amphibolite/greenshist	181.1±2.2	Mergozzo	Mulch et al., 2002
K–Ar	horneblende	stronalite	granulite	208±6	Cuzzago	McDowell and Schmid, 1968
K–Ar	biotite	metapelite	amphibolite	171±5	Bettola	McDowell and Schmid, 1968
K–Ar	biotite	metapelite	amphibolite	176±5	Albo	McDowell and Schmid, 1968
K–Ar	muscovite	metapelite	amphibolite	220±11	Candoglia	Hunziker, 1974
K–Ar	biotite	2 micas gneiss	amphibolite	190±10	Candoglia	Hunziker, 1974
K–Ar	biotite	metapelite	amphibolite	184±13	Candoglia	Wolff et al., 2012
K–Ar	biotite	stronalite	granulite	163±3	Cuzzago	Wolff et al., 2012
Rb–Sr	biotite	metapelite	amphibolite	172±13	Bettola	Jäger et al., 1967
Rb–Sr	biotite	2 micas gneiss	amphibolite	253±10	Megozzo	Hunziker 1974
Rb–Sr	biotite	stronalite	granulite	187±9	Anzola	Hunziker 1974
Rb–Sr	biotite	stronalite	granulite	185±15	Anzola	Hunziker 1974
Rb–Sr	biotite	biotite gneiss	amphibolite	180±7	Teglia	Hunziker 1974
Rb–Sr	biotite	2 micas gneiss	amphibolite	185±7	Candoglia	Hunziker 1974
Rb–Sr	biotite	stronalite	granulite	184	Anzola	Graeser and Hunziker, 1968
Rb–Sr	muscovite	pegmatite	amphibolite	180±7	Candoglia	Graeser and Hunziker, 1968
Rb–Sr	muscovite	pegmatite	amphibolite	236±10	Candoglia	Graeser and Hunziker, 1968

* Ages not reported in the Fig. 2 and/or 3.

Table 2 - Representative compilation of Triassic-Jurassic geochronological data available for the Strona di Omegna valley.

Dating method	Mineral	Rock type	Metamorphic facies	Age±error (Ma)	Locality	Reference
Sm–Nd Isochron	whole rock, plagioclase, garnet, orthopyroxene	stronalite	granulite	227±3	Forno	Voshage et al., 1987*
weigheted-mean $^{206}Pb/^{238}U$	zircon	dunite	granulite	200.5±0.3	La Balma-Monte Capio	Denyszyn et al., 2018*
weigheted-mean $^{206}Pb/^{238}U$	zircon	pyroxenite	granulite	200.1±0.5	La Balma-Monte Capio	Denyszyn et al., 2018*
$^{206}Pb/^{238}U$	rutile	Garnetiferous leucosome	granulite	176±4	Forno	Ewing et al., 2015
$^{206}Pb/^{238}U$	rutile	Garnetiferous leucosome	granulite	163±6	Forno	Ewing et al., 2015
$^{206}Pb/^{238}U$	rutile	Garnetiferous leucosome	granulite	175±4	Forno	Ewing et al., 2015
$^{206}Pb/^{238}U$	rutile	Garnetiferous leucosome	granulite	175±4	Forno	Ewing et al., 2015
$^{206}Pb/^{238}U$	rutile	layered metapelite restite and leucosome	granulite	164±3	Piana di Forno	Ewing et al., 2015
$^{206}Pb/^{238}U$	rutile	layered metapelite restite and leucosome	granulite	140±2	Piana di Forno	Ewing et al., 2015
$^{206}Pb/^{238}U$	rutile	layered metapelite restite and leucosome	granulite	175±5	Piana di Forno	Ewing et al., 2015
$^{206}Pb/^{238}U$	rutile	layered metapelite restite and leucosome	granulite	159±4	Piana di Forno	Ewing et al., 2015
$^{206}Pb/^{238}U$	rutile	stronalite	granulite	191-182±2	Forno	Smye et al., 2019
^{40}Ar-^{39}Ar	hornblende	mafic granulite	granulite	201.7±13	Campello Monti	Siegesmund et al., 2008
^{40}Ar-^{39}Ar	hornblende	mafic granulite	granulite	210.3±4.4	Campello Monti	Siegesmund et al., 2008
^{40}Ar-^{39}Ar	hornblende	mafic granulite	granulite	206.1±3	Piana di Forno	Siegesmund et al., 2008
^{40}Ar-^{39}Ar	hornblende	amphibolites	granulite	211.1±7	Forno	Siegesmund et al., 2008
^{40}Ar-^{39}Ar	hornblende	amphibolites	granulite	222.7±12.5	Otra	Siegesmund et al., 2008
^{40}Ar-^{39}Ar	hornblende	amphibolites	granulite	221.6±1.2	Rosarolo	Siegesmund et al., 2008
^{40}Ar-^{39}Ar	hornblende	amphibolites	amphibolite	240±20	Rosarolo	Siegesmund et al., 2008
^{40}Ar-^{39}Ar	hornblende	amphibolites	amphibolite	239.3±4.6	Road Rosarolo-Marmo	Siegesmund et al., 2008
^{40}Ar-^{39}Ar	hornblende	amphibolites	amphibolite	250.4±3.7	Fornero	Siegesmund et al., 2008
^{40}Ar-^{39}Ar	hornblende	mafic granulite	granulite	242±1	Piana di Forno	Boriani and Villa, 1997
^{40}Ar-^{39}Ar	hornblende	mafic granulite	granulite	217±1	Forno	Boriani and Villa, 1997
^{40}Ar-^{39}Ar	hornblende	amphibolite	amphibolite	243±1	Marmo	Boriani and Villa, 1997
K–Ar	biotite	stronalite	granulite	156.3±3.3	Campello Monti	Siegesmund et al., 2008
K–Ar	biotite	stronalite	granulite	159±3.4	Campello Monti	Siegesmund et al., 2008
K–Ar	biotite	stronalite	granulite	158.7±3.3	Road Campello Monti-Piana di Forno	Siegesmund et al., 2008
K–Ar	biotite	stronalite	granulite	175.7±3.7	Otra	Siegesmund et al., 2008
K–Ar	biotite	stronalite	granulite	166.6±3.5	Rosarolo	Siegesmund et al., 2008
K–Ar	biotite	stronalite	granulite	169.8±3.6	Rosarolo	Siegesmund et al., 2008
K–Ar	biotite	metapelite	amphibolite	183.3±3.8	Road Rosarolo-Marmo	Siegesmund et al., 2008
K–Ar	biotite	metapelite	amphibolite	167.3±3.5	Road Rosarolo-Marmo	Siegesmund et al., 2008
K–Ar	biotite	metapelite	amphibolite	179.1±3.8	Marmo	Siegesmund et al., 2008
K–Ar	biotite	metapelite	amphibolite	185.5±3.9	Fornero	Siegesmund et al., 2008
K–Ar	biotite	metapelite	amphibolite	201.7±4.2	Strona	Siegesmund et al., 2008
K–Ar	biotite	metapelite	amphibolite	200.3±4.2	Loreglia	Siegesmund et al., 2008
K–Ar	biotite	metapelite	amphibolite	231.6±4.8	Loreglia	Siegesmund et al., 2008
Rb–Sr	biotite	stronalite	granulite	193±68	Forno	Hunziker, 1974

* Ages not reported in the Fig. 2 and/or 3.

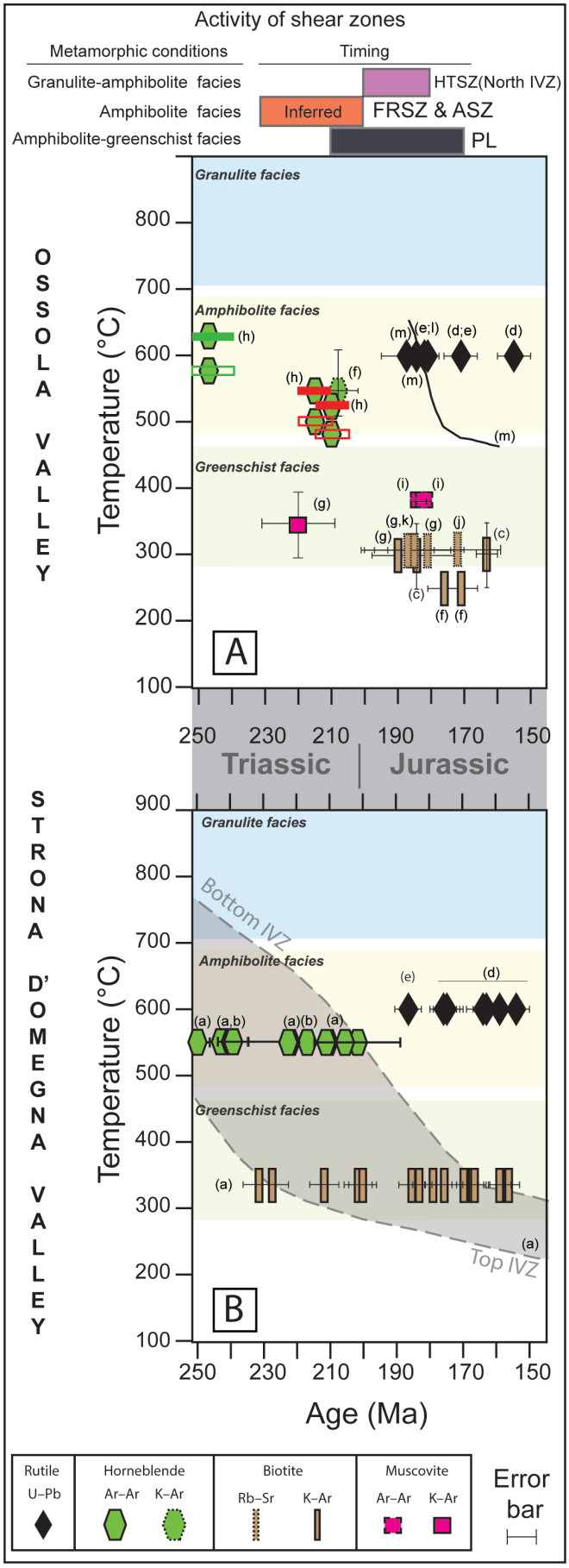

Ossola Valley

In the past decades, several radiometric studies were published for the basement rocks exposed in the Ossola valley (Fig. 3A). However, geochronological investigations dealing with U-Pb dating of zircon and/or monazite are rare (Koppel, 1974; Klötzli et al., 2014; Kusiak et al., 2019) and there is a lack of sampling continuity along the crustal section. Generally, both zircon and monazite provided Carboniferous/Permian ages suggesting that mafic sills locally intruded during Carboniferous (i.e., Albo sill of Klötzli et al., 2014; Fig. 2A) and that metamorphic growth/recrystallization of both zircon and monazite occurred during Early Permian as commonly found in rocks from IVZ (e.g., Vavra et al., 1999; Ewing et al., 2013; Klötzli et al., 2014). Despite the Anzola shear zone attracted many structural, microstructural, and geochemical studies (Brodie, 1981; Brodie et al., 1989; Brodie and Rutter, 1987; Altenberger, 1997, Stünitz, 1998; Rutter and Brodie, 1990; Rutter et al., 1993; 2007), the age of deformation is still poorly constrained.

Brodie et al. (1989) provided a direct attempt to date the Anzola shear zone by hornblende Ar-Ar dating. They obtained a minimum age of about 247 Ma for the unsheared metagabbro, whereas the shear zone provided two ages at 215±5 Ma, for the coarse-grained amphibole fraction, and 210±5 Ma, for the finer grained amphibole fraction (Fig. 3A). The authors provided also closure temperature estimates for the radiometric data considering the grain sizes and two cooling rates at 1 and 10°C/Ma, respectively (Fig. 3A). They stated that their results are consistent with pre-existing age determination considering a cooling rate of about 4°C/Ma. According to Brodie et al. (1989), the obtained ages record cooling because the blocking temperature was interpreted to be grain-size dependent, i.e., younger ages were obtained from the fine-grained syn-kinematic hornblende. Thus, according to the authors, the shearing was probably older than Late Triassic and likely it initiated prior to 280 Ma (i.e., prior to Early Permian). These Ar-Ar data were reinterpreted as possible evidence for an Late Triassic activity of the shear zone (Beltrando et al., 2015; Ewing et al., 2015).

Fig. 3 - Triassic-Jurassic T-t diagrams based on published radiometric data for Ossola (A) and Strona di Omegna (B) valleys. Both temperature and geochronological data are plotted according to the data as reported in the text or figures of the relative refences. In (A) six Ar-Ar hornblende data with relative error bars are shown and refer to three analysed samples but calculated using closure temperature for Ar in hornblende at cooling rates of 1 (unfilled error bars) and 10°C/Ma (filled error bars) according to Brodie et al. (1989); the data with green error bars refer to the undeformed gabbro whereas those with red error bars are associated to the hornblende from sheared metabasic rocks (for more details see Brodie et al., 1989). The black line associated to rutile UPb data represents the best-fit thermal history based on U-Pb rutile depth profile dating after Smye and Stockli (2014). In (B), the light grey area encloses the thermal history from base to top of the IVZ, after Siegesmund et al. (2008) and was depicted based on hornblende Ar-Ar and biotite K-Ar data. On the top of the figure the metamorphic conditions and timing for the activity of different shear zones is shown: the high-temperature shear zone (HTSZ)f rom north IVZ is from Langone et al. (2018); the low grade Pogallo Line (PL) is after Wolff et al. (2012). For the Forno-Rosarolo (FRSZ) and Anzola (ASZ) shear zones the inferred timing is based on this geochronological review and is in agreement with previous studies (e.g., Ewing et al., 2015).
References: a- Siegesmund et al., 2008; b- Boriani and Villa, 1997; c- Wolff et al., 2012; d- Ewing et al., 2015; e- Smye et al., 2019; f- McDowell and Schmidt, 1968; g- Hunziker, 1974; h- Brodie et al., 1989; i- Mulch et al., 2002; j- Jäger et al., 1967; k- Graeser and Hunziker, 1968; l- Zack et al., 2011; m- Smye and Stockli, 2014.

Other direct dating or (re)interpretations of mylonites from the Anzola shear zone are lacking. Nevertheless, we continue the review of the available geochronological-thermochronological data across the Ossola valley. Triassic ages in the Ossola valley are rare (Fig. 3A; Table 1). Rb-Sr cooling ages for muscovite at 243±10 Ma and 236±10 Ma were reported by Hunziker (1974) and Graeser and Hunziker (1968), respectively, for pegmatites near Candoglia (Fig. 2A). These cooling ages relative to pegmatitic samples are not shown in Fig. 3A since do not represent metamorphic events. Other Late Triassic ages (Fig. 3A) are reported for a two-micas gneiss in Candoglia (K-Ar muscovite age at 220±11 Ma; Hunziker, 1974) and for a metabasite in granulite-facies conditions (hornblende K-Ar age at 208±6 Ma; McDowell and Schmid, 1968). Since the first radiometric studies on the metamorphic rocks, the (Early-Middle) Jurassic interval is more frequently represented with respect to Triassic one. Several Rb-Sr biotite dates are available for different rock types along the valley (Fig. 2A) and span from 187±9 to 172±13 Ma (Fig. 3A; Jäger et al., 1967; Graeser and Hunziker, 1968; Hunziker, 1974). K-Ar dating of biotite within both amphibolite- and granulite-facies metapelites were carried out by several authors (McDowell and Schmid, 1968; Hunziker, 1974, Wolff et al., 2012) and range from 190±10 to 171±5 Ma (Fig. 3A). The most recent K-Ar biotite ages are presented by Wolff et al. (2012) for metamorphic rocks showing both amphibolite- and granulite-facies metamorphism. Biotite in granulites gave an age of 163±3 Ma, whereas biotite in amphibolite-facies rocks resulted older than ~ 20 Myr (184±13 Ma). According to Wolff et al. (2012), these ages should represent the activity of the PL during Jurassic crustal thinning.

The PL was already investigated in detail by Mulch et al. (2002). They dated three distinct populations of muscovite by Ar-Ar method for a sample collected close to the Ossola valley (Fig. 2A). Separates of undeformed muscovite porphyroclasts formed an Ar-Ar age plateau of ~ 182 Ma (Fig. 3A). Deformed muscovite and fine-grained muscovite provided the same average age (148±5 and 147±7 Ma, respectively) by *in-situ* Ar-Ar analyses. In addition, the authors obtained a relatively young Ar-Ar biotite age of 123±7 Ma. According to Mulch et al. (2002), the radiometric data obtained for undeformed porphyroclasts reflect the age of greenschist-facies mylonitization (occurred at about 380-400°C) along the PL. The younger ages were interpreted by the authors as an evidence of slow cooling rate during the Late Jurassic and Early Cretaceous.

The Ossola valley was sampled several times in the last decade for rutile U-Pb thermochronological studies (Figs. 2A and 3A; Zack et al., 2011; Smye and Stockli, 2014; Ewing et al., 2015; Smye et al., 2019). Zack et al. (2011) provided LA-ICP-MS age of 181±4 Ma for a rutile collected in a stronalite near the Premosello village. Smye and Stockli (2014) reported LA-ICP-MS U-Pb rutile ages from two stronalites collected between Anzola and Premosello. The U-Pb ages for these samples point to 184±5 Ma and 187±8 Ma, respectively. Ewing et al. (2015) performed U-Pb SHRIMP analyses on rutile separates and obtained two different age populations at 171±5 and 155±5 Ma, respectively. The older population was attributed by the authors to a first cooling event below 550-650°C. The presence of a younger population was interpreted as rapid reheating followed by renewed cooling.

Kusiak et al. (2019) have recently studied zircon from high-grade felsic mylonitic metapelites near Premosello (Fig. 2A). The isotopic data indicate old detrital cores and Permian metamorphic ages (280±4 Ma). Interestingly, the authors obtained also Triassic $^{206}Pb/^{238}U$ dates that they did not consider in the age calculations due to high common Pb. Kusiak et al. (2019) highlighted only the presence of one strongly deformed detrital core zircon yielding an apparent Jurassic U-Pb age (185 Ma) that they tentatively attributed to deformation.

Strona di Omegna Valley

Several authors tried to depict the T-t evolution of the IVZ crustal section exposed in the Strona di Omegna valley by collecting thermochronological data (e.g., Siegesmund et al., 2008). The well constrained tectono-metamorphic evolution of the crustal section exposed along this valley benefits also of numerous and detailed geochronological studies (Henk et al., 1997; Vavra et al., 1999; Ewing et al., 2013; Guergouz et al., 2018; Kunz et al., 2018). Generally, U-Pb monazite data are clustered around 275-280 Ma (Henk et al., 1997; Guergouz et al., 2018) and, according to Henk et al. (1997) they become systematically younger (from 292 to 276 Ma) towards the highest metamorphic grade.

A large age spread was documented for U-Pb zircon data, which provided useful information from prograde to retrograde metamorphic conditions (Vavra et al., 1999; Ewing et al., 2013; Klötzli et al., 2014; Guergouz et al., 2018; Kunz et al., 2018). Kunz et al. (2018) studied zircon grains from several samples (mostly metapelites and metapsammites) showing P-T conditions ranging from amphibolite- to granulite-facies. The authors obtained a spread of the U-Pb zircon dates > 60 Myr, from about 316 to 240 Ma. They recognized that in granulite-facies rocks there is a general decoupling of zircon chemical and isotopic signatures, i.e. no correlations were observed between U-Pb dates and internal features, Th/U ratio or Ti-in-zircon concentration. According to the authors, this decoupling is most likely due to the more intense thermal imprint (higher T for longer period) experienced by granulites with respect to amphibolite-facies samples. Noteworthy, the authors studied zircon grains from a mylonitic sample belonging to the Forno-Rosarolo shear zone. They recognized zircon internal features typical for growth at high temperature conditions with local evidence for late-stage fluid-induced recrystallization. This sample gave an overall range of U-Pb dates from 316 to 264 Ma and, according to the authors, it was the only one showing a correlation between U-Pb dates and geochemical data. Other zircon bearing samples from Val Strona di Omegna were studied by Vavra et al. (1999). They dated zircon grains from three different metapelitic samples representative of upper amphibolite- and granulite-facies zones and of the transition between these two sectors (Fig. 2B). Interestingly, the authors obtained a Late Permian age at 253±4 Ma for a high-U zircon domain from the transition zone and Early Triassic - Late Permian dates from altered zircon domains of both the transition zone (248±5 Ma, mean of 6 analyses) and the granulitic sample (246±12 Ma and 256±9 Ma). According to these authors, since Pb-loss from high-U zircon domains is dominantly controlled by the susceptibility of the crystal lattice, the rejuvenated ages do not necessarily correspond to a geological event. However, the occurrence of several young apparent ages from U-rich domains also from other localities of the IVZ led the authors to suggest that they were the result of a near-complete resetting during an episode of annealing. Analogously, the youngest apparent ages from altered domains of zircon from the Strona di Omegna valley coincide within error with those reported from altered domains in other valleys of the IVZ. According to the Vavra et

al. (1999), this coincidence and the fact that they are slightly younger than the youngest apparent ages from high-U domains would suggest that a major episode of zircon alteration and partial resetting occurred because of a strong thermal and/or decompression event at 249±7 Ma. This event was linked by the authors to the Permian post-collisional strike-slip tectonics, basin formation and volcanism. It is interesting to note that Vavra et al. (1999) reported also a further recrystallization process induced by fluid ingression within zircon grains from other localities of the IVZ. Zircon domains associate to this late stage provided Late Triassic/Early Jurassic dates and were associated with alkaline magmatism and hydrothermal activity due to the onset of continental breakup of Pangea.

Middle-Late Triassic ages were obtained also by Boriani and Villa (1997) dating hornblende (Ar-Ar method) from three metabasites showing amphibolite/granulite-facies conditions (Figs. 2B and 3B). According to the authors, two samples gave indistinguishable ages, i.e., at 243 and 242±1 Ma, whereas the sample collected from an intermediate position between the other two (Fig. 2B), provided a younger date at 217±1 Ma, likely related to local fluid-induced recrystallization. Ar-Ar amphibole dates ranging from late Permian to Late Triassic are also reported by Siegesmund et al. (2008) for samples collected along all the valley for both the IVZ and adjacent SdL unit (Figs. 2B and 3B). Hornblende ages showed an east-west age gradient decreasing from 257±1 Ma, near the CMB Line, to 202±3 Ma, close to the Insubric Line (Fig. 2B). Recently, Denyszyn et al. (2018) reported zircon U-Pb ages at the Triassic-Jurassic boundary (about 200 Ma) for the La Balma-Monte Capio mafic/ultramafic intrusion (Fig. 2B). The authors interpreted the age as indicative of a short-lived magmatic system associated with the Central Atlantic Magmatic Province, which is related to the opening of the central Atlantic Ocean and thus the breakup of Pangaea. However, it is interesting to note that mafic rocks from the same locality (Monte Capio sill) were previously dated at Carboniferous (Klötzli et al., 2014). As reported by Berno et al. (2019) it cannot be excluded that the Triassic-Jurassic age obtained by Denyszyn et al. (2018) represents the product of zircon recrystallization rather than the age of magmatic crystallization. As highlighted by Berno et al. (2019) it has been demonstrated that the prolonged residence under high-temperature conditions for the deep sectors of the IVZ produced perturbation of the U-Pb isotope system in zircons, thereby leading to apparent age rejuvenation (e.g., Vavra et al. 1999; Zanetti et al., 2016; Kunz et al., 2018).

Several thermochronological data based on U-Pb dating of rutile are available in the literature for granulite-facies metapelites from the base of the IVZ in the Strona di Omegna valley (Ewing et al., 2013; 2015; Smye et al., 2019; Figs. 2B and 3B). Rutile crystallized during Permian granulite-facies conditions and provided Jurassic U-Pb ages indicating cooling through 650-550°C. Recently, Smye et al. (2019) dated rutile from a garnet-rich metapelite that was already studied for geochemical characterization by Luvizotto et al. (2009). Rutile provided $^{206}Pb/^{238}U$ spot dates in the range of 182-191 Ma. Ewing et al. (2015) obtained two age peaks: the main one at ~ 160 Ma and a subordinate one at ~ 175 Ma (Fig. 3B). According to the authors the younger age cluster (~ 160 Ma) coincides with the exhumation of sub-continental mantle to the floor of the Alpine Tethys and thus can be interpreted as regional cooling following a short heating episode recorded by the distal Adriatic margin. The ~ 175 Ma age was interpreted by the authors as the cooling in the footwall of rift-related faults and shear zones.

The rutile U-Pb ages (Ewing et al., 2013; 2015; Smye et al., 2019) partially overlap the biotite K-Ar ages obtained from the base of the IVZ by Siegesmund et al. (2008; Fig. 3B). These authors recognized that the biotite K-Ar dates decrease from 230 to 156 Ma moving toward lower crustal levels, running subparallel to the hornblende ages but at lower temperatures (Fig. 3B). Siegesmund et al. (2008) did not observe any abrupt offset of the decreasing age profile across the two tectonic lineaments located in the lower part of the profile, i.e. the CMB and the PL, suggesting that Mesozoic tectonics affected the entire basement pile in a uniform way.

DISCUSSIONS AND CONCLUSIONS

Timing of the Forno-Rosarolo and Anzola shear zones

As it concerns the deformation age of the Forno-Rosarolo shear zone, a robust interpretation is still lacking as well as direct attempts to date shearing. Siegesmund et al. (2008), following the work of Henk et al. (1997), reconstructed the T-t curves of both the IVZ and the adjacent SdL by using geochronological and thermochronological data collected along the Strona di Omegna valley. As shown in the plot of the Ar-Ar hornblende data (Fig. 7 of Siegesmund et al., 2008), the isochron ages show a well-defined progression becoming younger towards the Insubric Line. The authors reported that samples comprised between the Insubric Line and the Forno-Rosarolo shear zone did not provide a true plateau and that they were affected by a considerable amount of excess argon that makes the obtained ages unreliable. However, some of these samples provided well-defined isochrons with an average isochron age of 208±2 Ma that was not linked to the ductile deformation. Interestingly, Boriani and Villa (1997) also obtained a younger Ar-Ar hornblende date from the sample coming from the Forno-Rosarolo area with respect to the other two samples that they collected structurally above and below this sector. The authors interpreted the younger age as due to local fluid-induced recrystallization of hornblende. It is interesting to note that three mafic granulites collected by Siegesmund et al. (2008) close to the Forno village (Fig. 2B) gave ages between 211 and 222 Ma comparable to the one obtained by Boriani and Villa (1997) in the same area (217±1 Ma). Since the Boriani and Villa (1997) young age was interpreted as linked to fluid induced recrystallization, it is likely that this process influenced also the data provided by Siegesmund et al. (2008) from the same area, even if these latter authors did not discuss this hypothesis.

As reported in the review above, a direct attempt to the date the Anzola shear zone was carried out by Brodie et al. (1989). According to the authors, the high temperature shear zone started prior to 280 Ma, probably around 300 Ma, and recorded a period of crustal thinning and cooling of more than 100 Myr of duration. Several authors provided an alternative interpretation for the Brodie et al. (1989) age dataset. According to Beltrando et al. (2015) and Ewing et al. (2015), a different scenario would be that the younger ages record Late Triassic deformation-induced recrystallisation and not diffusive loss of Ar. As already suggested by Boriani and Villa (1997), it appears that Ar-Ar ages of amphiboles in the IVZ are not controlled only by diffusive loss of Ar and that recrystallization of hornblende also plays an important role. Actually, the hypothesis suggested by Beltrando et al. (2015) and Ewing et al. (2015) was already proposed by Brodie and

Rutter (1987) considering only existing geochronological and thermochronological data at that time, without the Ar-Ar data set from the Anzola shear zone. The authors stated that *"an alternative possibility exists that high-temperature extensional faulting in the Ivrea Zone could be at least coeval with the earlier part of the movements on the Pogallo Fault (i.e., 230-180 Ma). We remain unable at this time satisfactorily to resolve the conflicting temperature/age estimates for the Ivrea Zone which arise from consideration of the radiometric age data, and the stratigraphic data which constrains the age of movements on the Pogallo Fault*" (Schmid et al., 1987). This alternative interpretation has been recently reinforced by the dating of high temperature deformation in metagabbros from the northernmost sector of the IVZ (Finero area, Langone et al., 2018). The authors performed U-Pb zircon dating for mylonites and ultramylonites showing granulite- to upper amphibolite-facies deformation conditions. According to their zircon dating and Ar-Ar ages (Boriani and Villa, 1997) from deformed hornblende grains from the shear zone, Langone et al. (2018) proposed that the high temperature shearing occurred during Late Triassic and ended during Early Jurassic (about 183 Ma) under amphibolite-facies conditions.

A recent indirect dating of high temperature deformation during Early Jurassic has been also provided by Corvò et al. (2020) for mylonites and ultramylonites developed within the mantle rocks of the Finero area. These authors found a single zircon grain (187 Ma) within the fine-grained matrix of a peridotitic ultramylonite, which they interpreted as an inherited grain from Triassic-Jurassic felsic dykes (e.g., Schaltegger et al., 2015) partially affected by the high temperature shear zone.

In summary, even though the evidences of the activity of syn-rift shear zones in the available geochronological datasets from the Strona di Omegna and Ossola valleys were not always considered or even recognized in the past, several recent investigations indicate that some of those ages were linked to deformation (e.g., Beltrando et al., 2015; Ewing et al., 2015; Langone et al., 2018; Petri et al., 2019; Corvò et al., 2020).

Up to now mylonites from the two investigated shear zones were (directly or indirectly) only dated by Ar-Ar hornblende method. As reported in a recent review dealing with geochronology of shear zones (Oriolo et al. 2018), the coupling of thermochronologic and geochronological data of mylonitic belts and associated intrusions and/or adjacent blocks is mandatory in order to reconstruct detailed P-T-D-t paths of shear zones and neighbouring areas. In addition, the growing knowledge on other geochronometers and advances in microanalytical techniques, such as the laser ablation split-stream (allowing to collect simultaneously chemical and isotopic data, e.g., Kylander-Clark et al., 2013) or the LA-ICP-MS/MS dating (allowing to perform on line removal of isobaric interferences, e.g., *in situ* Rb-Sr dating; Zack and Hogmalm, 2016) offer the possibility to constrain the timing of shearing using other mineral phases and isotopic systems. In particular, U-Pb dating of syn-kinematic titanite can be performed for mylonites derived from mafic protoliths (e.g., Storey et al., 2004; Papapavlou et al., 2017; Giuntoli et al., 2020), whereas monazite can be dated *in situ* within metapelitic-derived mylonites (e.g., Montomoli et al., 2013; Carosi et al., 2020; Simonetti et al., 2020a; 2020b). Analogously, other syn-kinematic (e.g., biotite) or slickenfibre (e.g., K-feldspar, illite, calcite and albite) minerals can be dated *in situ* by Rb-Sr method (e.g., Tillberg et al., 2020).

Triassic-Jurassic T-t evolution

In the last decades the T-t evolution of the IVZ has been depicted in several studies and continuously updated by considering new geochronological and thermochronological data (e.g. Hunziker, 1974, Schmid et al., 1989; Brodie et al., 1989; Zingg et al., 1990; Siegesmund et al., 2008; Smye and Stockli, 2014; Ewing et al., 2015). Furthermore, tables summarizing the available radiometric data, fission track ages and/or the sedimentary records comprising also the Triassic-Jurassic interval, have been compiled in the recent years (e.g., Vavra et al, 1999; Peressini et al., 2007; Zanetti et al., 2013; Beltrando et al., 2015). In this section we focus on geochronological and thermochronological data for the Triassic-Jurassic interval published for the Strona di Omegna and Ossola valleys (Fig. 3). The T-t evolution for both the upper and lower part of the IVZ exposed along the Strona di Omegna section was reconstructed in detail by Siegesmund et al. (2008) by using hornblende Ar-Ar data and biotite K-Ar data. According to Siegesmund et al. (2008), the obtained ages decreasing towards the rocks of a formerly deeper crustal position simply reflect slow exhumation and cooling during Triassic (Fig. 3B), after the Permian heating caused by the lower crustal mafic intrusion. The authors highlighted only an apparent change of the cooling rate from more than 4°C/Ma (4.6°C/Ma and 4.9°C/Ma for the base and the top of the IVZ, respectively) during Triassic to about 1°C/Ma during Jurassic (Fig. 3B). These cooling curves were not influenced by recrystallization due to the activity of the main tectonic discontinuities in the valley (e.g., the PL and the CMB Line). The decreasing trend obtained by Siegesmund et al. (2008) do not fit with the reconstruction proposed by Boriani and Villa (1997). Based on their three amphibole ages representative of different crustal levels, the authors proposed that the entire Strona di Omegna section did not experience a differential exhumation later than 240 Ma and only a local fluid induced recrystallization in the intermediate portion was recognised.

For the Ossola valley, Schmid et al. (1989) suggested a T-t path based on published radiometric data (U-Pb, Rb-Sr, K-Ar; Fig. 3A). The same data were used also by Brodie et al. (1989) and integrated with new Ar-Ar ages on hornblende from the Anzola unsheared metagabbro and adjacent mafic mylonites (Fig. 3A). The authors stated that their new data were broadly consistent with the existing radiometric constraints. It is worth to note that there is no T-t path available for the Ossola valley since the dataset is made of data derived from a discontinuous sampling and using different methods with respect to the dataset of the Strona di Omegna section (Fig. 2A *vs* 2B and Fig. 3A *vs* 3B).

In both reconstructions of Fig. 3, it is interesting to note the position of the U-Pb thermochronological data obtained from rutile in the granulites. As reported before, rutile in the IVZ has been studied by several authors (Zack et al., 2011; Smye and Stockly, 2014; Ewing et al., 2015; Smye et al., 2019) and the thermochronological data indicate that granulitic rocks recorded temperature of about 600°C during Early-Middle Jurassic. According to Smye et al. (2019), the IVZ underwent conductive heating of > 100°C prior to the initiation of mantle exhumation and crustal excision around 180 Ma during Tethyan extension. The authors proposed that the heating occurred on two different timescales, in particular: i) a conductive heating over 10^7 yr due to mantle thinning preceding crustal exhumation and ii) advecting heating over < 10^5 yr by local invasion of hot fluids when ambient temperatures were 500°C. Since the first study on rutile U-Pb

data, it seems that the Jurassic heating event affected only the granulitic rocks comprised between the studied shear zones and the deepest levels of the continental crust (i.e., towards the Insubric Line). It is interesting to note that the same heating event has not been recorded at higher crustal levels (amphibolite-facies lithologies) otherwise a partial or total reset of other geochronometers and thermochronometers would be observed in these crustal portions. All these data indicate that the heating was recorded at regional scale (see Beltrando et al., 2015) but it probably affected mainly the high-grade rocks (stronalites), formerly at the base of the IVZ. A wider heating affecting also the amphibolite-facies rocks is not apparent from the thermochronological data available for these levels of the continental crust since the biotite and muscovite radiometric ages do not show a total or partial resetting (Fig. 3). Alternatively, the overlap between U-Pb rutile ages from granulites and thermochronological data (e.g., Rb-Sr, Ar-Ar and K-Ar of micas; Fig. 3) from upper crustal rocks would suggest a fast cooling during Jurassic induced by a rapid exhumation of the whole crustal section (e.g., Beltrando et al., 2015). This period of rapid exhumation of the IVZ broadly corresponds with the activity of shear zones at different crustal levels (Fig. 3). A fast exhumation process has been already suggested for the Adria lithosphere (e.g., Malenco area, Müntener et al., 2000).

In both the Strona di Omegna and Ossola valleys, the deformation is notably not limited to the Forno-Rosarolo and Anzola shear zones. Indeed, in the lowermost part of the crustal profiles other high temperature and pseudotachylite-bearing mylonitic belts are exposed (e.g., Techmer et al., 1992). As suggested by Pittarello et al. (2012) such a deformation probably occurred during the early Mesozoic crustal extension, prior to the Alpine orogeny. Even if further studies are needed, it cannot be excluded that also the shear heating (e.g., Brun and Cobbold, 1980; Mako and Caddick, 2018) contributed at least partially to the temperature increment in this sector of the crust concurrently with other heat sources (i.e., asthenosphere upwelling and hot fluids; Smye et al., 2019). Hence, the potential effect of rift-related deformation and heating should be considered in the interpretation of thermochronological datasets of the IVZ, in particular for those sectors representing portions of the lower crust and/or adjacent to shear zones. New detailed investigations and acquisition of new data able to directly constrain the timing and tectono-thermal activity of these structures would confirm their role and possible hierarchy in crustal thinning processes during Tethyan rifting.

CONCLUSIONS

The present geochronological and thermochronological review allows to shed light on the evidences of Triassic-Jurassic rift-related deformation in the fossil Adriatic margin of the Alpine Tethys exposed along two valleys of the Ivrea-Verbano Zone. The data review highlighted that: i) the two valleys have been sampled several times but with a different detail; ii) geochronological and thermochronological studies are rarely focused on shear zones; iii) the direct attempt to date deformation has been done by Ar-Ar method; iv) local evidences for fluid-induced recrystallization of both geo- and thermo-chronometers during Late Triassic-Early Jurassic have been reported for both crustal sections; v) these recrystallization processes have been interpreted as evidence for rift-related deformation; v) granulites recorded Early-Middle Jurassic heating and cooling events that apparently did not affect the lower grade metamorphic rocks of the upper crustal levels. We emphasise that more detailed investigations of the shear zones are needed in order to better understand the rifting processes that occurred at the fossil Adriatic margin during Triassic-Jurassic extension and exhumation. We finally propose that the shear zones subject of this review must be investigated by applying a modern multidisciplinary approach combining detailed fieldwork, microstructural analyses, petrochronology and thermochronology.

ACKNOWLEDGEMENTS

This manuscript is dedicated to Marco Beltrando, a teacher to some, a colleague to others, certainly a great scientist and a friend to everyone. He dedicated part of his research activities on the shear zones presented here. This research was funded by the following project: PRIN2017 “Micro to Macro - how to unravel the nature of the large magmatic events (20178LPCPW- Langone Antonio)”. The manuscript has been conceptualized by L.A. and all the authors equally contributed to the original initial draft and writing. We thank Benoît Petri and an anonymous reviewer for their comments that improved the quality of the manuscript. We also thank the associate editor Riccardo Tribuzio for his comments and editing.

REFERENCES

Altenberger U., 1995. Local disequilibrium of plagioclase in high-temperature shear zones of the Ivrea Zone, Italy. J. Metam. Geol., 13 (5): 553-558.

Altenberger U., 1997. Strain localization mechanisms in deep-seated layered rocks. Geol. Rundsch., 86 (1): 56-68.

Aravadinou E. and Xypolias P., 2017. Evolution of a passive crustal-scale detachment (Syros, Aegean region): Insights from structural and petrofabric analyses in the hanging-wall. J. Struct. Geol., 103: 57-74. https://doi.org/10.1016/j.jsg.2017.09.008.

Beltrando M., Manatschal G., Mohn G., Dal Piaz G.V., Vitale Brovarone A. and Masini E., 2014. Recognizing remnants of magma-poor rifted margins in high-pressure orogenic belts: The Alpine case study. Earth. Sci. Rev., 131: 88-115. https://doi.org/10.1016/j.earscirev.2014.01.001.

Beltrando M., Stockli D.F., Decarlis A. and Manatschal G., 2015. A crustal-scale view at rift localization along the fossil Adriatic margin of the Alpine Tethys preserved in NW Italy. Tectonics, 34: 1927-1951. https://doi.org/10.1002/2015TC003973.

Berno D., Tribuzio R., Zanetti A. and Hémond C., 2019. Evolution of mantle melts intruding the lowermost continental crust: constraints from the Monte Capio-Alpe Cevia mafic-ultramafic sequences (Ivrea-Verbano Zone, Northern Italy). Contrib Miner. Petrol, 175 (1): 1-28. https://doi.org/10.1007/s00410-019-1637-8.

Bertotti G., Picotti V., Bernoulli D. and Castellarin A., 1993. From rifting to drifting: tectonic evolution of the South-Alpine upper crust from the Triassic to the Early Cretaceous. Sedim. Geol., 86: 53-76. https://doi.org/10.1016/0037-0738(93)90133-P.

Boriani A. and Villa I.M., 1997. Geochronology of regional metamorphism in the Ivrea-Verbano Zone and Seri e dei Laghi, Italian Alps. Schweiz. Miner. Petrogr., 77: 381-402. https://doi.org/10.5169/SEALS-58492.

Boriani A., Burlini L. and Sacchi R., 1990. The Cossato-Mergozzo-Brissago Line and the Pogallo Line (Southern Alps, Northern Italy) and their relationships with the late-Hercynian magmatic and metamorphic events. Tectonophysics, 182: 91-102.

Brodie K.H., 1981. Variation in amphibole and plagioclase composition with deformation. Tectonophysics, 78: 385-402. https://doi.org/10.1016/0040-1951(81)90021-4.

Brodie K.H. and Rutter E.H., 1987. Deep crustal extensional faulting in the Ivrea Zone of Northern Italy. Tectonophysics, 140: 193-212. https://doi.org/10.1016/0040-1951(87)90229-0.

Brodie K.H., Rutter E.H. and Rex D., 1989. On the age of deep crustal extensional faulting in the Ivrea zone, Northern Italy. Geol. Soc. London Spec. Publ., 45: 203-210. https://doi.org/10.1144/GSL.SP.1989.045.01.11.

Brun J.P. and Cobbold P.R., 1980. Strain heating and thermal softening in continental shear zones: a review. J. Struct. Geol., 2: 149-158.

Carosi R., Montomoli C. and Iaccarino S., 2018. 20 years of geological mapping of the metamorphic core across Central and Eastern Himalayas. Earth Sci. Rev., 177: 124-138. https://doi.org/10.1016/j.earscirev.2017.11.006.

Carosi R., Petroccia A., Iaccarino S., Simonetti M., Langone A. and Montomoli C., 2020. Kinematics and timing constraints in a transpressive tectonic regime: The example of the Posada-Asinara Shear Zone (NE Sardinia, Italy). Geosciences, 10: 288. https://doi.org/10.3390/geosciences10080288.

Corvò S., Langone A., Padrón-Navarta J.A., Tommasi A. and Zanetti A., 2020. Porphyroclasts: Source and sink of major and Trace Elements during deformationinduced metasomatism (Finero, Ivrea-Verbano Zone, Italy). Geosciences, 10: 196. https://doi.org/10.3390/geosciences10050196.

Decarlis A., Beltrando M., Manatschal G., Ferrando S. and Carosi R., 2017. Architecture of the distal Piedmont-Ligurian rifted margin in NW Italy: hints for a flip of the rift system polarity. Tectonics, 36: 2388-2406. https://doi.org/10.1002 /2017TC004561.

Degli Alessandrini G., 2018. Deformation mechanisms and strain localization in the mafic continental lower crust. PhD thesis, School Geogr. Earth Environ. Sci. Univ. Plymouth, 366 pp.

Denyszyn S.W., Fiorentini M.L. Maas R and Dering G., 2018. A bigger tent for CAMP. Geology, 46 (9): 823-826.

Ewing T.A., Hermann J. and Rubatto D., 2013. The robustness of the Zr-in-rutile and Ti-in-zircon thermometers during high-temperature metamorphism (Ivrea-Verbano Zone, Northern Italy). Contrib. Miner. Petrol., 165: 757-779. https://doi.org/10.1007/s00410-012-0834-5.

Ewing T.A., Rubatto D., Beltrando M. and Hermann J., 2015. Constraints on the thermal evolution of the Adriatic margin during Jurassic continental break-up: U-Pb dating of rutile from the Ivrea-Verbano Zone, Italy. Contrib. Miner. Petrol., 169: 44. https://doi.org/10.1007/s00410-015-1135-6.

Ferrando S., Bernoulli D. and Compagnoni R., 2004. The Canavese zone (internal Western Alps): a distal margin of Adria. Schweiz. Miner. Petrogr. Mitt., 84: 237-256.

Fossen H. and Cavalcante G.C.G., 2017. Shear zones - A review. Earth Sci. Rev., 171: 434-455. https://doi.org/10.1016/j.earscirev.2017.05.002.

Garde A.A., Boriani A. and Sørensen E.V., 2015. Crustal modelling of the Ivrea-Verbano zone in Northern Italy re-examined: Coseismic cataclasis versus extensional shear zones and sideways rotation. Tectonophysics, 662: 291-311.

Giorgis S., Michels Z., Dair L., Braudy N. and Tikoff B., 2017. Kinematic and vorticity analyses of the western Idaho shear zone, USA. Lithosphere, 9 (2): 223-234.

Giuntoli F., Menegon L., Warren C.J., Darlin, J. and Anderson M.W., 2020. Protracted shearing at midcrustal conditions during large-scale thrusting in the Scandinavian Caledonides. Tectonics, 39: e2020TC006267. https://doi.org/10.1029/2020TC006267.

Graeser S. and Hunziker J.C., 1968. Rb-Sr und Pb-Isotopen-Bestimmungen an Gesteinen und Mineralien der Ivrea-Zone. Schweiz. Miner. Petrogr., 48: 189-204.

Guergouz C., Martin L., Vanderhaeghe O., Thébaud N. and Fiorentini M., 2018. Zircon and monazite petrochronologic record of prolonged amphibolite to granulite facies metamorphism in the Ivrea-Verbano and Strona-Ceneri Zones, NW Italy. Lithos, 308-309: 1-18. https://doi.org/10.1016/j.lithos.2018.02.014.

Hartmann G. and Hans Wedepohl K., 1993. The composition of peridotite tectonites from the Ivrea Complex, Northern Italy: Residues from melt extraction. Geochim. Cosmochim. Acta, 57: 1761-1782. https://doi.org/10.1016/0016-7037(93)90112-A.

Henk A., Franz L., Teufel S. and Oncken O., 1997. Magmatic underplating, extension, and crustal reequilibration: Insights from a cross-section through the Ivrea Zone and Strona-Ceneri Zone, Northern Italy. J. Geol., 105: 367-378. https://doi.org/10.1086/515932.

Hodges K.V. and Fountain D.M., 1984. Pogallo Line, South Alps, Northern Italy: An intermediate crustal level, low-angle normal fault? Geology, 12 (3): 151-155.

Hunziker J.C., 1974. Rb-Sr and K-Ar age determination and the Alpine tectonic history of the Western Alps. Mem. Ist. Geol. Miner. Univ. Padova, 31: 54.

Iaccarino S., Montomoli C., Carosi R., Massonne H.-J., Langone A. and Visonà D., 2015. Pressure-temperature-time deformation path of kyanite-bearing migmatitic paragneiss in the Kali Gandaki valley (Central Nepal): Investigation of Late Eocene-Early Oligocene melting processes. Lithos, 231: 103-121. https://doi.org/10.1016/j.lithos.2015.06.005.

Iacopini D., Carosi R., Montomoli C. and Passchier C.W., 2008. Strain analysis and vorticity of flow in the Northern Sardinian Variscan Belt: Recognition of a partitioned oblique deformation event. Tectonophysics, 446: 77-96. https://doi.org/10.1016/j.tecto.2007.10.002.

Jäger E., Niggli E. and Wenk E., 1967.Rb-Sr-Altersbestimmungen an Glimmern der Zentralalpen. Beitr Geol Karte Schweiz, NF 134: 67

Karakas O., Wotzlaw J.F., Guillong M., Ulmer P., Brack P., Economos R., Bergantz G.W., Sinigoi S. and Bachmann O., 2019. The pace of crustal-scale magma accretion and differentiation beneath silicic caldera volcanoes: Geology, 47: 719-723.

Kenkmann T., 2000. Processes controlling the shrinkage of porphyroclasts in gabbroic shear zones. J. Struct. Geol., 22: 471-487. https://doi.org/10.1016/S0191-8141(99)00177-7.

Kenkmann T. and Dresen G., 2002. Dislocation microstructure and phase distribution in a lower crustal shear zone - an example from the Ivrea-Zone, Italy. Int. J. Earth Sci., 91 (3): 445-458.

Klötzli U.S., Sinigoi S., Quick J.E., Demarchi G., Tassinari C.C.G., Sato K. And Günes Z., 2014. Duration of igneous activity in the Sesia Magmatic System and implications for high-temperature metamorphism in the Ivrea–Verbano deep crust. Lithos, 206–207: 19-33.

Koppel V., 1974. Isotopic U-Pb ages of monazites and zircons from the crust-mantle transition and adjacent units of the Ivrea and Ceneri Zones (Southern Alps, Italy). Contrib. Miner. Petrol., 43: 55-70.

Kozur H., 1991. The evolution of the Meliata-Hallstatt ocean and its significance for the early evolution of the Eastern Alps and Western Carpathians. Palaeo. Palaeo. Palaeo., 87: 109-135. https://doi.org/10.1016/0031-0182(91)90132-B.

Kunz B.E., Johnson T.E., White R.W. and Redler C., 2014. Partial melting of metabasic rocks in Val Strona di Omegna, Ivrea Zone, Northern Italy. Lithos, 190-191, 1-12. https://doi.org/10.1016/j.lithos.2013.11.015.

Kunz B.E., Regis D. and Engi M., 2018. Zircon ages in granulite facies rocks: decoupling from geochemistry above 850°C? Contrib. Miner. Petrol., 137: 26. https://doi.org/10.1007/s00410-018-1454-5.

Kusiak M.A., Kovaleva E., Wirth R., Klötzli U., Dunkley D.J., Yi K. and Lee S., 2019. Lead oxide nanospheres in seismically deformed zircon grains. Geochim. Cosmochim. Acta, 262: 20-30.

Kylander-Clark A., Hacker B. and Cottle J.M., 2013. Laser ablation split-stream ICP petrochronology. Chem. Geol., 345: 99-112.

Langone A., Zanetti A., Daczko N.R., Piazolo S., Tiepolo M. and Mazzucchelli M., 2018. Zircon U-Pb dating of a lower crustal shear zone: A case study from the northern sector of the Ivrea-Verbano Zone (Val Cannobina, Italy). Tectonics, 37: 322-342. https://doi.org/10.1002/2017TC004638.

Law R.D., 2014. Deformation thermometry based on quartz c-axis fabrics and recrystallization microstructures: A review. J. Struct. Geol., 66: 129-161. https://doi.org/10.1016/j.jsg.2014.05.023.

Law R.D., Searle M.P. and Simpson R.L., 2004. Strain, deformation temperatures and vorticity of flow at the top of the Greater Himalayan Slab, Everest Massif, Tibet. J. Geol. Soc. London, 161: 305-320.

Luvizotto G.L., Zack T., Meyer H.P., Ludwig T., Triebol S., Kronz A., Münker C., Stockli D.F., Prowatke S., Klemme S., Jacob D.E. and von Eynatten H., 2009. Rutile crystals as potential trace element and isotope mineral standards for microanalysis. Chem. Geol., 261 (3-4): 346-369.

Mako C.A. and Caddick M.J., 2018. Quantifying magnitudes of shear heating in metamorphic systems. Tectonophysics, 744: 499-517.

Manatschal G., Müntener O., Lavier L.L., Minshull T.A. and Péron-Pinvidic G., 2007. Observations from the Alpine Tethys and Iberia-Newfoundland margins pertinent to the interpretation of continental breakup. Geol. Soc. London Spec. Publ., 282: 291-324. https://doi.org/10.1144/SP282.14.

McDowell F.W. and Schmid R., 1968. Potassium-argon ages from the Valle d'Ossola section of the Ivrea-Verbano Zone (Northern Italy). Schweiz. Miner. Petrogr., 48: 205-210.

Mohn G., Manatschal G., Beltrando M., Masini E. and Kusznir N., 2012. Necking of continental crust in magma-poor rifted margins: Evidence from the fossil Alpine Tethys margins: necking of continental crust. Tectonics, 31 (1): TC1012. https://doi.org/10.1029/2011TC002961.

Mohn G., Manatschal G., Müntener O., Beltrando M. and Masini E., 2010. Unravelling the interaction between tectonic and sedimentary processes during lithospheric thinning in the Alpine Tethys margins. Int. J. Earth. Sci., 99: 75-101. https://doi.org/10.1007/s00531-010-0566-6.

Montomoli C., Iaccarino S., Carosi R., Langone A. and Visonà D., 2013. Tectonometamorphic discontinuities within the Greater Himalayan Sequence in Western Nepal (Central Himalaya): Insights on the exhumation of crystalline rocks. Tectonophysics, 608: 1349-1370. https://doi.org/10.1016/j.tecto.2013.06.006.

Mulch A., Rosenau M., Dörr W. and Handy M.R., 2002. The age and structure of dikes along the tectonic contact of the Ivrea-Verbano and Strona-Ceneri Zones (Southern Alps, Northern Italy, Switzerland). Schweiz. Miner. Petrogr., 82: 55-76.

Müntener O., Hermann J. and Trommsdorff V., 2000. Cooling history and exhumation of lower-crustal granulite and upper mantle (Malenco, eastern central Alps). J. Petrol., 41: 175-200.

Oriolo S., Wemmer K., Oyhantçabal P., Fossen H., Schulz B. and Siegesmund S., 2018. Geochronology of shear zones - A review. Earth Sci. Rev., 185: 665-683.

Papapavlou K., Darling J.R., Storey C.D., Lightfoot P.C., Moser D.E. and Lasalle S., 2017. Dating shear zones with plastically deformed titanite: New insights into the orogenic evolution of the Sudbury impact structure (Ontario, Canada). Precambr. Res., 291: 220-235. https://doi.org/10.1016/j.precamres.2017.01.007.

Parsons A.J., Coleman M.J., Ryan J.J., Zagorevski A., Joyce N.L., Gibson H.D. and Larson, K.P., 2018. Structural evolution of a crustal-scale shear zone through a decreasing temperature regime: The Yukon River shear zone, Yukon-Tanana terrane, Northern Cordillera. Lithosphere, 10 (6): 760-782. https://doi.org/10.1130/L724.1.

Peressini G., Quick J.E., Sinigoi S., Hofmann A.W. and Fanning M., 2007. Duration of a large mafic intrusion and heat transfer in the lower crust: a SHRIMP U-Pb Zircon study in the Ivrea-Verbano Zone (Western Alps, Italy). J. Petrol., 48: 1185-1218. https://doi.org/10.1093/petrology/egm014.

Petri B., Duretz T., Mohn G., Schmalholz S.M., Karner G.D. and Müntener O., 2019. Thinning mechanisms of heterogeneous continental lithosphere. Earth Planet Sci. Lett., 512: 147-162. https://doi.org/10.1016/j.epsl.2019.02.007.

Pittarello L., Pennacchioni G. and Di Toro G., 2012. Amphibolite-facies pseudotachylytes in Premosello metagabbro and felsic mylonites (Ivrea Zone, Italy). Tectonophysics, 580, 43-57.

Real C., Froitzheim N., Carosi R. and Ferrando S., 2018. Evidence of large-scale Mesozoic detachments preserved in the basement of the Southern Alps (northern Lago di Como area). Italy. J. Geosci., 137: 283-293. https://doi.org/10.3301/IJG.2018.15.

Redler C., Johnson T.E., White R.W. and Kunz B.E., 2012. Phase equilibrium constraints on a deep crustal metamorphic field gradient: metapelitic rocks from the Ivrea Zone (NW Italy): Ivrea Zone metamorphic field gradient. J. Metam.. Geol., 30: 235-254. https://doi.org/10.1111/j.1525-1314.2011.00965.x.

Rutter E.H. and Brodie K.H., 1990. Some geophysical implications of the deformation and metamorphism of the Ivrea zone, Northern Italy. Tectonophysics, 182 (1-2): 147-160.

Rutter E.H., Brodie K.H. and Evans P.J., 1993. Structural geometry, lower crustal magmatic underplating and lithospheric stretching in the Ivrea-Verbano zone, northern Italy. J. Struct. Geol., 15: 647-662. https://doi.org/10.1016/0191-8141(93)90153-2.

Rutter E.H., Brodie K.H., James T. and Burlini L., 2007. Large-scale folding in the upper part of the Ivrea-Verbano Zone, NW Italy. J. Struct. Geol., 29: 1-17. https://doi.org/10.1016/j.jsg.2006.08.013.

Schaltegger U., Ulianov A., Muntener O., Ovtcharova M., Peytcheva I., Vonlanthen P., Vennemann T., Antognini M. and Girlanda F., 2015. Megacrystic zircon with planar fractures in miaskite-type nepheline pegmatites formed at high pressures in the lower crust (Ivrea Zone, southern Alps, Switzerland). Amer. Miner., 100: 83-94.

Schmid S.M., 1993. Ivrea zone and adjacent southern Alpine basement. In: J.F. Raumer and F. Neubauer (Eds.). Pre-Mesozoic geology in the Alps, Springer, Berlin, Heidelberg, p. 567-583.

Schmid S.M., Aelbi H.R., Heller F. and Zingg A., 1989. The role of the Periadriatic Line in the tectonic evolution of the Alps. Geol. Soc. London Spec. Publ., 45 (1):135-171.

Schmid R. and Wood B.J., 1976. Phase relationships in granulitic metapelites from the Ivrea-Verbano zone (Northern Italy). Contrib. Miner. Petrol., 54: 255-279. https://doi.org/10.1007/BF00389407.

Schmid S.M., Zingg A. and Handy M., 1987. The kinematics of movements along the Insubric Line and the emplacement of the Ivrea Zone. Tectonophysics, 135 (1-3): 47-66.

Schuster R., Stüwe K., 2008. Permian metamorphic event in the Alps. Geology, 36: 603-606. https://doi.org/10.1130/G24703A.1.

Sibson R.H., 1977. Fault rocks and fault mechanisms. J. Geol. Soc. London, 133: 191-213.

Siegesmund S., Layer P., Dunkl I., Vollbrecht A., Steenken A., Wemmer K. and Ahrendt H., 2008. Exhumation and deformation history of the lower crustal section of the Valstrona di Omegna in the Ivrea Zone, southern Alps. Geol. Soc. London Spec. Publ., 298: 45-68. https://doi.org/10.1144/SP298.3.

Simonetti M., Carosi R., Montomoli C., Corsini M., Petroccia A., Cottle J.M. and Iaccarino S., 2020a. Timing and kinematics of flow in a transpressive dextral shear zone, Maures Massif (Southern France). Int. J. Earth. Sci., 109: 2261-2285. https://doi.org/10.1007/s00531-020-01898-6.

Simonetti M., Carosi R., Montomoli C., Cottle J.M. and Law R.D., 2020b. Transpressive deformation in the southern European Variscan Belt: New insights from the Aiguilles Rouges Massif (Western Alps). Tectonics, 39. https://doi.org/10.1029/2020TC00615.

Smye A.J. and Stockli D.F., 2014. Rutile U-Pb age depth profiling: A continuous record of lithospheric thermal evolution. Earth Planet. Sci. Lett., 408: 171-182. https://doi.org/10.1016/j.epsl.2014.10.013.

Smye A.J., Lavier L.L., Zack T. and Stockli D.F., 2019. Episodic heating of continental lower crust during extension: A thermal modeling investigation of the Ivrea-Verbano Zone. Earth Planet. Sci. Lett., 521: 158-168.

Speranza F., Minelli L., Pignatelli A. and Chiappini M., 2012. The Ionian Sea: The oldest in situ ocean fragment of the world? Magnetic modelling of the Ionian Sea. J. Geophys. Res. Solid Earth, 117. https://doi.org/10.1029/2012JB009475.

Storey C.D., Brewer T.S. and Parrish R.R., 2004. Late-Proterozoic tectonics in northwest Scotland: one contractional orogeny or several? Precambr. Res. 134 (3-4), 227-247. http://dx.doi.org/10.1016/j.precamres.2004.06.004.

Stünitz H., 1998. Syndeformational recrystallization - dynamic or compositionally induced? Contrib. Miner. Petrol., 131: 219-236. https://doi.org/10.1007/s004100050390.

Techmer K.S., Ahrendt H. and Weber K., 1992. The development of pseudotachylyte in the Ivrea-Verbano Zone of the Italian Alps. Tectonophysics, 204: 307-322.

Tillberg M., Drake H., Zack T., Kooijman E., Whitehouse M.J. and Åström M.E., 2020. In situ Rb-Sr dating of slickenfibres in deep crystalline basement faults. Sci Rep 10: 562. https://doi.org/10.1038/s41598-019-57262-5.

Vavra G., Schmid R. and Gebauer D., 1999. Internal morphology, habit and U-Th-Pb microanalysis of amphibolite-to-granulite facies zircons: geochronology of the Ivrea Zone (Southern Alps). Contrib. Miner. Petrol., 13 4(4): 380-404.

Wolff R., Dunkl I., Kiesselbach G., Wemmer K. and Siegesmund S., 2012. Thermochronological constraints on the multiphase exhumation history of the Ivrea-Verbano Zone of the Southern Alps. Tectonophysics, 579: 104-117. https://doi.org/10.1016/j.tecto.2012.03.019.

Wu W., Liu J., Zhang L., Qi Y. and Ling C., 2017. Characterizing a middle to upper crustal shear zone: Microstructures, quartz c-axis fabrics, deformation temperatures and flow vorticity analysis of the northern Ailao Shan-Red River shear zone, China. J. Asian Earth Sci., 139: 95-114. https://doi.org/10.1016/j.jseaes.2016.12.026.

Xypolias P., 2010. Vorticity analysis in shear zones: A review of methods and applications. J. Struct. Geol., 32: 2072-2092. https://doi.org/10.1016/j.jsg.2010.08.009.

Zack T., Stockli D.F., Luvizotto G.L., Barth M.G., Belousova E., Wolfe M.R. and Hinton R.W., 2011. In situ U-Pb rutile dating by LA-ICPMS: 208Pb correction and prospects for geological applications. Contrib. Miner. Petrol., 162: 515-530.

Zack T., Hogmalm J., 2016. Laser ablation Rb/Sr dating by online chemical separation of Rb and Sr in an oxygen-filled reaction cell. Chem. Geol., 437: 120-133

Zanetti A., Mazzucchelli M., Sinigoi S., Giovanardi T., Peressini G. and Fanning M., 2013. SHRIMP U-Pb zircon Triassic intrusion age of the Finero mafic complex (Ivrea-Verbano Zone, Western Alps) and its geodynamic implications. J. Petrol., 54 (11): 2235-2265.

Zanetti A., Giovanardi T., Langone A., Tiepolo M., Wu F.-Y., Dallai L. and Mazzucchelli M., 2016. Origin and age of zircon-bearing chromitite layers from the Finero phlogopite peridotite (Ivrea-Verbano Zone, Western Alps) and geodynamic consequences. Lithos, 262: 58-74.

Zhang Q., Giorgis S. and Teyssier C., 2013. Finite strain analysis of the Zhangbaling metamorphic belt, SE China - Crustal thinning in transpression. J. Struct. Geol., 49: 13-22. https://doi.org/10.1016/j.jsg.2013.01.008.

Zingg A., 1980. Regional metamorphism in the Ivrea Zone (Southern Alps, N-Italy): field and microscopic Investigations. Schweiz Miner. Petrogr. Mitt., 60:153-179.

Zingg A., 1983. The Ivrea and Strona-Ceneri zones (Southern Alps, Ticino and N-Italy) - a revew. Schweiz Miner. Petrogr. Mitt., (2-3): 361-392.

Zingg A., 1990. The Ivrea crustal cross-section (Northern Italy and Southern Switzerland). In: M.H. Salisbury and D.M. Fountain (Eds.), Exposed cross-sections of the continental crust. Springer Netherlands, Dordrecht, p. 1-19. https://doi.org/10.1007/978-94-009-0675-41.

Zingg A., Handy M.R., Hunziker J.C. and Schmid S.M., 1990. Tectonometamorphic history of the Ivrea Zone and its relationship to the crustal evolution of the Southern Alps. Tectonophysics, 182: 169-192. https://doi.org/10.1016/0040-1951(90)90349-D.

Received, February 11, 2021
Accepted, May 19, 2021